Pedestal Structure Model Tests

J.D. Callen, University of Wisconsin, Madison, WI 53706-1609
J.M. Canik, Oak Ridge National Laboratory, Oak Ridge, TN 37831

U.S. Transport Task Force Workshop, General Atomics, San Diego, CA, April 6–9, 2011

Theses:

1) The paleoclassical-based pedestal structure model[1] makes predictions for profiles of n_e, $dT_e/d\rho$ and Ω_t in the pedestal and pedestal height β_e^{ped}.

2) Recent tests of the model predictions have been encouraging:
quantitative "point" comparisons[1] with DIII-D 98889 pedestal data,[2]
SOLPS modeling results for DIII-D 98889 pedestals and NSTX w/wo Li.[3]

3) Progress is being made on proposed tests:[1] 4 fundamental, 4 secondary.

Outline:

Motivation — what do we want to predict and why?

Predictions of pedestal structure model

Profile and point tests — for DIII-D 98889 pedestal and NSTX

Progress on proposed tests

---

[1]J.D. Callen, "A Model of Pedestal Transport," report UW-CPTC 10-6, August 30, 2010, available via `http://www.cptc.wisc.edu`.

[2]J.D. Callen, R.J. Groebner, T.H. Osborne, J.M. Canik, L.W. Owen, A.Y. Pankin, T. Rafiq, T.D. Rognlien and W.M. Stacey, "Analysis of pedestal transport," Nuclear Fusion **50**, 064004 (2010).

[3]J.M. Canik et al., "Edge transport and turbulence reduction with lithium coated plasma facing components in the National Spherical Torus Experiment," invited paper JI2 1 at the 2010 Chicago APS-DPP meeting (paper submitted to Phys. Plasmas).

Pedestal Quickly Reaches Quasi-Equilibrium; Top Evolves

- **Pedestal evolves between ELMs:**

  pedestal gradients in $0.98 < \Psi_N < 1.0$ region are same at 6–9 & 60–63 ms,

  but top of pedestal ($0.85 < \Psi_N < 0.98$) evolves from 6–9 to 60–63 ms,

  due to core-edge coupling as the core plasma recovers after the ELM,

  and ultimately precipitates an ELM.

- **"Pedestal structure" here means:**

  profiles of n_e, T_e and Ω_t in the $0.98 \lesssim \Psi_N \leq 1$ region.

- **Key pedestal structure features to be addressed in this talk are:**

  n_e mostly "aligned" with T_e profile,

  but n_e top slightly outside T_e top,

  $dT_e/d\rho \simeq$ constant in pedestal.

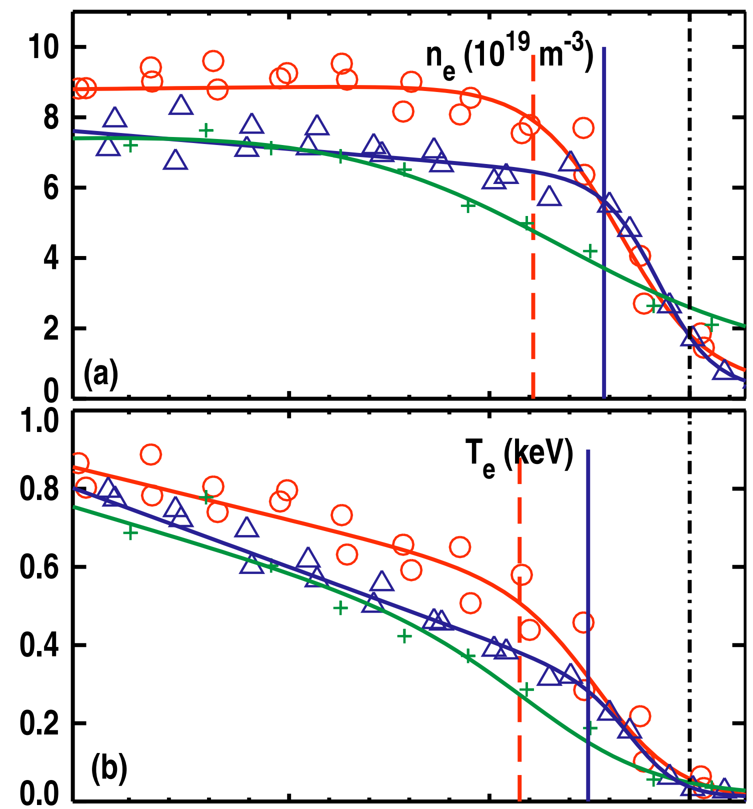

Figure 1: **Temporal evolution of n_e, T_e edge profiles ($0.85 < \Psi_N < 1.01$) for 0–3 (+), 6–9 (△) and 60–63 (○) ms after an ELM. Vertical solid (dashed) lines show "top" of pedestal at 6–9 (60–63) ms. Adapted from Fig. 8 of Groebner et al., Nucl. Fusion 49, 045013 (2009).**

Motivation: What Are Key Issues For Pedestal Structure?

1) How does huge electron heat flux from core get carried through the low n_e, T_e pedestal? Answer: by making $|dT_e/d\rho|$ very large $\Longrightarrow$ T_e pedestal.

Conductive electron heat flow (Watts) through a flux surface (S) is $P_e \simeq n_e \chi_e \, S \left(-\dfrac{dT_e}{d\rho}\right)$.

The needed T_e gradient in the pedestal is thus $-\dfrac{dT_e}{d\rho} \equiv \dfrac{T_e}{L_{T_e}} = \dfrac{P_e}{n_e \chi_e S}$.

$P_e \sim \dfrac{\overline{n_e T_e}\, V}{\tau_E}$ plus $\tau_E \sim \dfrac{a^2}{\overline{\chi}_e}$ yields $\dfrac{a}{L_{Te}} \sim \dfrac{\overline{n_e T_e}}{n_e^{\rm ped} T_e^{\rm ped}} \gg 10$ if $\overline{\chi}_e \sim \chi_e^{\rm ped}$.

Paleoclassical $\chi_e^{\rm pc} \sim$ agreed with interpretive χ_e in 98889 pedestal[2] and $\chi_e^{\rm pc}(\text{ped}) \sim \overline{\chi}_e$.

2) How does density build up so high with modest core fueling and mostly edge fueling (up steep pedestal density gradient!)? Answer: density pinch.

It has long been known that density pinches are important in H-mode pedestals.[4]

Interpretive Stacey-Groebner analysis[5] indicates inward pinch nearly cancels diffusion.

Paleoclassical model predicted density pinch and inferred diffusivity in 98889 pedestal.[2]

IN RESPONSE: A pedestal structure model based on paleoclassical transport was developed[1] for initial "quasi-saturation" — for $n_e(\rho)$, $T_e(\rho)$, $\Omega_t(\rho)$.

[4] M.E. Rensink, S.L. Allen, A.H. Futch, D.N. Hill, G.D. Porter and M.A. Mahdavi, "Particle transport studies for single-null divertor discharges in DIII-D," Phys. Fluids B **5**, 2165 (1993).

[5] W.M. Stacey and R.J. Groebner, "Interpretation of particle pinches and diffusion coefficients in the edge pedestal of DIII-D H-mode plasmas," Phys. Plasmas **16**, 102504 (2009).

Pedestal Plasma Transport Equations

- **Assumptions are made in order to develop the pedestal structure model:**[1]

  1) Paleoclassical transport dominates density and electron temperature transport in the pedestal, but anomalous transport is often dominant from top of pedestal into the core.

  2) Electron heating in the pedestal is small; heat mostly just flows out through pedestal.

  3) Density is fueled from the edge recycling ion source, perhaps plus NBI core fueling.

- **Thus, equilibrium electron density and energy conservation equations are:**

$$\langle \vec{\nabla}\cdot(\vec{\Gamma}^{\rm pc}+\vec{\Gamma}^{\rm an})\rangle = \langle S_n\rangle \quad \Longrightarrow \quad -\frac{1}{V'}\frac{d^2}{d\rho^2}(V'\bar{D}_\eta n_e)+\frac{1}{V'}\frac{d}{d\rho}(V'\Gamma^{\rm an}) = \langle S_n(\rho)\rangle,$$

$$\langle \vec{\nabla}\cdot(\vec{q}_e^{\,\rm pc}+\vec{q}_e^{\,\rm an}+\tfrac{5}{2}T_e\vec{\Gamma})\rangle = 0 \;\Longrightarrow\; -\frac{M+1}{V'}\frac{d^2}{d\rho^2}\left(V'\bar{D}_\eta\frac{3}{2}n_eT_e\right)+\frac{1}{V'}\frac{d}{d\rho}\left[V'(\Upsilon_e^{\rm an}+\frac{5}{2}T_e\Gamma)\right] = 0.$$

- **Neglecting anomalous density transport in the pedestal, the density equation can be integrated from ρ to the separatrix ($\rho = a$) to yield**

$$-\left[\frac{d}{d\rho}(V'\bar{D}_\eta n_e)\right]_\rho = \dot{N}(\rho), \qquad \text{\#/s of electrons flowing outward through the } \rho \text{ surface.}$$

- **Neglecting anomalous electron heat xport in pedestal and integrating yields**

$$-\left[\frac{d}{d\rho}\left(V'\bar{D}_\eta\frac{3}{2}n_eT_e\right)\right]_\rho = \hat{P}_e(\rho), \quad \text{effective electron power flow (W) through } \rho \text{ surface.}$$

Key Paleoclassical Parameter Is Magnetic Field Diffusivity D_η

- Magnetic field diffusivity is induced by parallel neoclassical resistivity $\eta_\parallel^{\rm nc}$:

$$\boxed{D_\eta \equiv \frac{\eta_\parallel^{\rm nc}}{\mu_0} = \frac{\eta_0}{\mu_0}\frac{\eta_\parallel^{\rm nc}}{\eta_0},} \quad \text{in which reference diffusivity is} \quad \boxed{\frac{\eta_0}{\mu_0} \equiv \frac{m_e \nu_e}{\mu_0 n_e e^2} \simeq \frac{1400\, Z_{\rm eff}}{[T_e({\rm eV})]^{3/2}}\frac{\ln\Lambda}{17}.}$$

- Ratio of neoclassical to reference ($\perp$) resistivity is approximately (for 98889)

$$\boxed{\frac{\eta_\parallel^{\rm nc}}{\eta_0} \simeq \frac{\eta_\parallel^{\rm Sp}}{\eta_0} + \frac{\mu_e}{\nu_e},} \quad \underbrace{\frac{\eta_\parallel^{\rm Sp}}{\eta_0} \simeq \frac{\sqrt{2}+Z_{\rm eff}}{\sqrt{2}+13Z_{\rm eff}/4}}_{\text{Spitzer } \simeq\, 0.4}, \quad \underbrace{\frac{\mu_e}{\nu_e} \simeq \frac{3.4}{1+\nu_{*e}^{1/2}+2\,\nu_{*e}}}_{\text{t.p. viscosity effect}}, \quad \underbrace{\nu_{*e} \equiv \frac{f_t/\epsilon^2}{1.46 f_c}\frac{\nu_e}{v_{Te}/R_0 q}}_{\text{collisionality}}.$$

- Basic scaling is $D_\eta \propto Z_{\rm eff}/T_e^{3/2}$ but viscosity effects due to large fraction of trapped particles ($f_t \simeq 0.77$) cause $\eta_\parallel^{\rm nc}/\eta_0$ to vary $\gtrsim$ 2 in 98889 pedestal:[2]

$$\frac{\eta_\parallel^{\rm nc}}{\eta_0} \simeq 0.4 \text{ (on separatrix)}, \simeq 0.64 \text{ (at pedestal mid-point)}, \simeq 0.81 \text{ (at pedestal top)}.$$

- For simplicity of notation the geometrically effective D_η will be written as

$$\boxed{\bar{D}_\eta \equiv \frac{a^2}{\bar{a}^2} D_\eta,} \quad \text{in which} \quad \frac{a^2}{\bar{a}^2} \equiv \frac{1}{\langle R^{-2}\rangle}\left\langle \frac{|\vec{\nabla}\rho|^2}{R^2}\right\rangle \simeq 1.6 \text{ in 98889 pedestal.}$$

Key Pedestal Structure Predictions Have Been Identified

- **Neglecting anomalous transport & edge recycling in the pedestal and integrating the particle, heat flow, Ω_t equations over ρ yields the predictions:**[1]

$$n_e \text{ profile:} \qquad n_e(\rho) \simeq \frac{n_e(\rho_{\mathrm{REF}})\, D_\eta(\rho_{\mathrm{REF}})}{D_\eta(\rho)} \propto \frac{T_e^{3/2}}{Z_{\mathrm{eff}}} \frac{\eta_0}{\eta_\parallel^{\mathrm{nc}}}, \tag{1}$$

$$T_e \text{ gradient:} \qquad -\frac{dT_e}{d\rho} = \frac{\text{electron power flow}}{(3/2)(V' \bar{D}_\eta n_e)} \sim \text{constant} \implies \chi_{e\,\mathrm{eff}}^{\mathrm{pc}} \simeq 1.2\, D_\eta, \tag{2}$$

$$\text{toroidal rotation:} \qquad \frac{d\Omega_t}{d\rho} \simeq 0 \implies \Omega_t(\rho) \simeq \text{constant} = \Omega_t(a) \text{ on separatrix.} \tag{3}$$

- **Here, the various variables and parameters are:**

  ρ is a toroidal-flux-surface-based radial coordinate,

  ρ_{REF} is a reference radius within the pedestal (e.g., at the separatrix or mid-point) and $V' \equiv dV(\rho)/d\rho = S(\rho)/\langle|\vec{\nabla}\rho|\rangle$ where $V(\rho)$, $S(\rho)$ are the volume, area of ρ flux surface.

- **Transition into ETG-driven anomalous radial electron heat transport in the core plasma determines the initial height of the electron pressure pedestal:**[1]

$$\beta_e^{\mathrm{ped}} \equiv \frac{n_e^{\mathrm{ped}} T_e^{\mathrm{ped}}}{B_0^2/2\mu_0} \sim \frac{3\sqrt{2}}{\pi f_\#} \frac{\eta_\parallel^{\mathrm{nc}}}{\eta_0} \frac{L_{T_e}}{R_0 q}, \ \text{for } \chi_e^{\mathrm{ETG}} \simeq f_\# \chi_e^{\mathrm{gB}},\ \ \chi_e^{\mathrm{gB}} = \frac{\varrho_e}{L_{T_e}} \frac{T_e}{eB},\ \ f_\# \sim 1.4\text{–}3. \tag{4}$$

- **Neutral fueling effects add a bit to the pedestal density, displace the n_e profile outward from the T_e profile and cause $d\Omega_t/d\rho < 0$ in the pedestal.**

First Tests Use Low Density DIII-D 98889 Pedestal Data[2]

- **Experimental data is fit by tanh (n_e, T_e) and spline (T_i) profiles.**

- **Radial coordinate used is $\rho \equiv \sqrt{\Phi/\pi B_{t0}}$ with $\rho_N \equiv \rho/a$.**

- **Key pedestal regions; positions:**

  I: core, $0.85 < \rho_N < 0.96$;
  pedestal "top" is at $\rho_t \simeq 0.96a$,

  II: top half, $0.96 < \rho_N < 0.98$;
  density mid-point is at $\rho_n \simeq 0.982a$,

  III: bottom half, $0.98 < \rho_N < 1.0$;
  separatrix is at $\rho_{sep} = a$.

- **Key pedestal profile features:**

  $n_e(\rho)$ nearly "aligned" with T_e profile,
  $dT_e/d\rho \simeq$ constant in pedestal,
  "top" of T_e pedestal hard to identify,
  $|dT_i/d\rho|$ is smallest gradient.

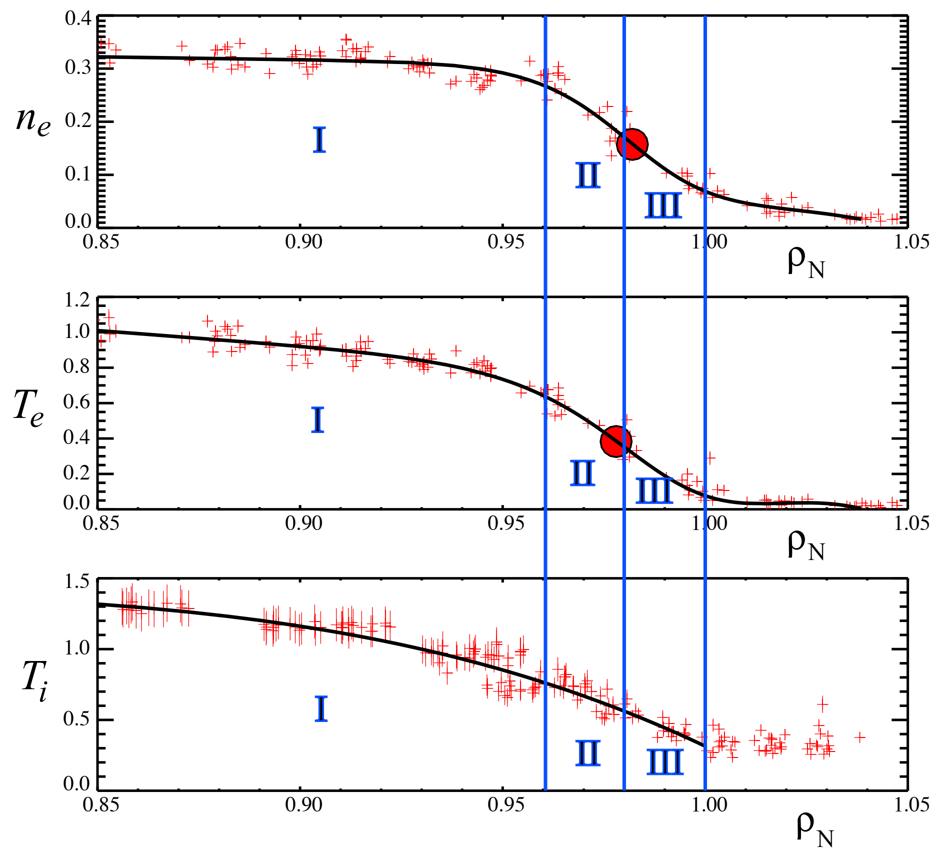

Figure 2: **Edge n_e, T_e & T_i profiles obtained averaging Thomson, CER data over 80–99% of average 33.53 ms between ELMs.[2] Lines show tanh & spline fits; ○ are fit symmetry points.**

Predictions for χ_e and n_e Profiles Agree In 98889 Pedestal[2]

- **$\chi_e(\rho)$ and $n_e(\rho)$ model predictions $\sim$ agree with interpretive SOLPS results[2] for various carbon transport models in the pedestal region $0.97 \lesssim \Psi_N < 1$.**
- **In core region ($\Psi_N \ll 0.97$) χ_e is much greater than paleoclassical χ_e — because of ETG-induced anomalous transport there? also, some D^{an}?**

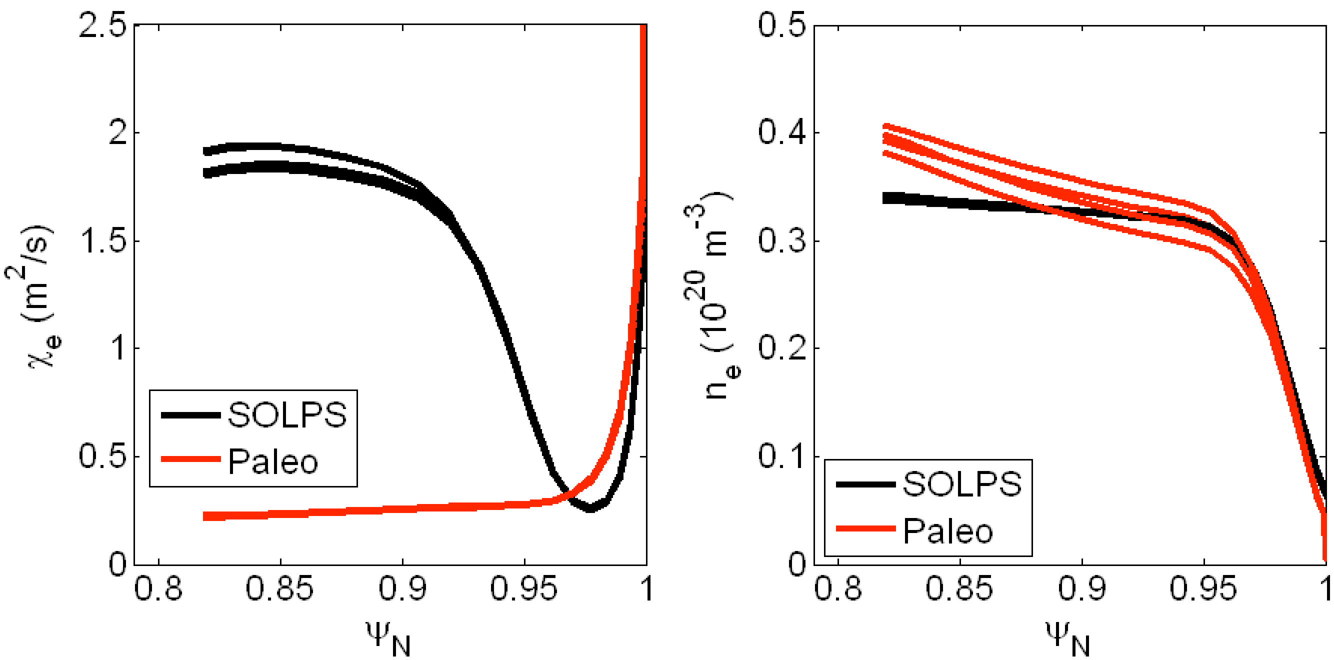

Figure 3: **Comparison of SOLPS interpretive modeling with $Z_{\text{eff}}(\rho)$ on DIII-D 98889 pedestal[2] to paleoclassical-based pedestal structure model predictions in edge plasma region.**

NSTX χ_e And n_e Pedestals[3] Captured By Model Predictions

- **Recent NSTX experiments have produced[3] very different H-mode pedestals w/wo Lithium on wall.**

- **Carbon density & $Z_{\rm eff}$ profiles for the two expts. are very different:**

  Pre-Li expt. similar to DIII-D pedestals;

  Post-Li expt. has higher carbon and $Z_{\rm eff}$ further into plasma — to $\Psi_N \lesssim 0.9$.

- **Notable features of these results:[3]**

  χ_e agrees in pedestals for both expts.;

  Pre-Li expt. χ_e is anomalous at and inside pedestal top ($\Psi_N < 0.95$);

  Post-Li expt. χ_e might be dominantly paleoclassical in edge (in to $\Psi_N \sim 0.8$);

  electron density profiles do not agree as well, but trends are captured.

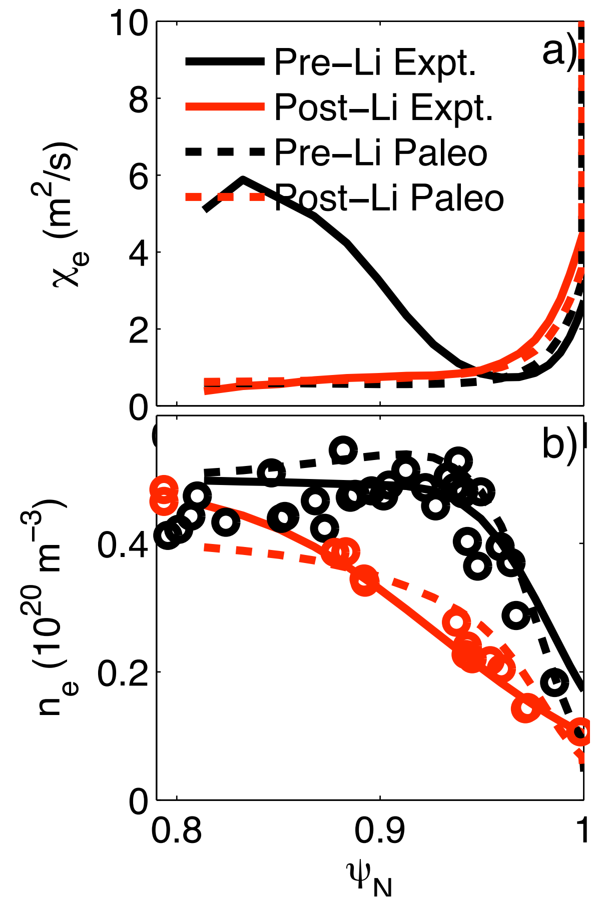

Figure 4: **Comparison of SOLPS interpretive modeling of NSTX pedestals[3] w/wo Lithium to paleoclassical-based pedestal structure model predictions in edge plasma region.**

Some Model Tests Have Been Made; Many More Are Needed

- **4 fundamental (F) tests of pedestal structure model have been proposed:[1]**

  #1: $n_e \sim 1/D_\eta$ — factor $\sim$ 1.5 difference in DIII-D 98889 and NSTX w/wo Li

  #2: $dT_e/d\rho \simeq$ constant in pedestal — most pedestals approximately exhibit this

  #3: $dT_e/d\rho \simeq \hat{P}_e/[(3/2)V'\bar{D}_\eta n_e]$ — DIII-D 98889 and NSTX w/wo Li agree $\chi_e \simeq 1.2\, D_\eta$

  #4: fluctuation-induced transport negligible in pedestal? — insufficient radial resolution

- **4 secondary (S) tests of pedestal structure model have been proposed:[1]**

  #1: n_e at top of pedestal — not always well predicted, too high by factor $\sim$ 2?

  #2: offset of n_e, T_e profiles proportional to fueling $\dot{N}$ — hints, but not yet tested

  #3: $\beta_e^{\rm ped}$ — in DIII-D 98889 pedestal model/expt. $\sim$ 0.84–1.8 (for $f_\# \sim 3 \searrow 1.4$)

  #4: $d\Omega_t/d\rho \sim -\dot{N}$ — hints of effect at high pedestal density and with high triangularity

- **Many more tests of the pedestal structure model predictions are needed:**

  quantitative tests, pedestal database (S. Smith, W-P11) — F #3, S #3 and S #2, S #4

  scaling tests for varying $Z_{\rm eff}$, $\hat{P}_e$, q, collisionality, shape — F #3, S #3 and S #2, S #4

  predictive modeling of pedestal density profile via paleo transport (A. Pankin, Edge-III)

Discussion: Sources Of Error And Pedestal Evolution

- **Determination of $D_\eta \propto f(\nu_{*e}) Z_{\rm eff}/T_e^{3/2}$ is critical but (factors $\lesssim 2$):**

  $Z_{\rm eff}$ is often assumed to be constant in pedestal[2] but should decrease toward separatrix (SOLPS modeling of 98889 estimates yield $Z_{\rm eff} \simeq 2.8,\ 2.6,\ 1.9$ at ρ_t, ρ_n, a).

  Present paleoclassical transport model is only accurate to within a factor of two.

  In paleoclassical theory D_η should be multiplied by fraction of $\psi_{\rm p}$ due to local $\langle \vec{J}\cdot\vec{B}\rangle$.

- **The $\beta_e^{\rm ped}$ prediction here is just for the initial, transport-limited pedestal height immediately after L-H transition or an ELM:**

  Pedestal should reach this state in $\tau \sim (2L_{Te})^2/\bar{D}_\eta$ ($\sim$ few ms for 98889 parameters[2]).

  Then, top of pedestal moves radially inward as core plasma re-equilibrates — but n_e and T_e profiles in the pedestal should remain fixed on the longer "global" τ_E time scale.

  Continuing growth and inward spreading of top of T_e profile eventually violates peeling-ballooning (PB) instability boundary and precipitates an ELM.

  If electron heat flow through pedestal $\hat{P}_e$ is too large, P-B limit could be exceeded before this "quasi-equilibrium" $\beta_e^{\rm ped}$ is reached — then T_e would rise linearly between ELMs.

  In this situation one would obtain more frequent Type I ELMs, perhaps accompanied by Type II ELMs if high-n ballooning limit is exceeded in bottom half of the pedestal.

Summary

- **The paleoclassical-based pedestal structure model[1] makes predictions for profiles of n_e, $dT_e/d\rho$ and Ω_t in the pedestal and pedestal height $\beta_e^{\rm ped}$:**

  Neglecting fueling, $n_e \sim 1/D_\eta$, $-\,dT_e/d\rho \simeq \hat{P}_e/[(3/2)V'\bar{D}_\eta n_e]$, $\Omega_t(\rho) \simeq$ const. in pedestal.

  Edge fueling adds to n_e, shifts n_e relative to T_e profile and causes $d\Omega/d\rho < 0$ in pedestal.

  Transition to ETG-induced transport at pedestal top can predict pedestal height $\beta_e^{\rm ped}$.

- **Recent tests of the model predictions have been encouraging:**

  quantitative "point" comparisons[1] with DIII-D 98889 pedestal data[2] within factor 1.5,

  SOLPS modeling of χ_e and n_e in DIII-D 98889 and NSTX w/wo Li[3] pedestals.

- **Progress is being made on proposed tests:[1] 4 fundamental, 4 secondary — but need tests on more data sets, scaling tests and predictive modeling.**

- **Additional notes:**

  Predictions are for the "initial" pedestal structure and height, whose top then evolves.

  Paleoclassical transport is a minimum transport level; adding other transport processes weakens the pedestal gradients (particularly of density) and increases the pedestal width.

Pedestal Electron Density Profile

- **Integrating density flow equation from ρ surface to separatrix ($\rho = a$) yields[1]**

$$n_e(\rho)\,\bar{D}_\eta(\rho)\,V'(\rho) \;=\; n_e(a)\,\bar{D}_\eta(a)V'(a) \;+\; \int_\rho^a d\hat{\rho}\,\dot{N}_e(\hat{\rho}).$$

- **However, fueling effect from $\dot{N}$ is often small in pedestal:**

$$\frac{\int_{\rho_n}^a d\hat{\rho}\,\dot{N}_e(\hat{\rho})}{[n_e\bar{D}_\eta V']_{\rho_n}} \simeq \frac{(a-\rho_n)\,\dot{N}_e[(a+\rho_n)/2]}{n_e(\rho_n)\,\bar{D}_\eta(\rho_n)\,V'(\rho_n)} \simeq 0.06 \ll 1 \qquad \text{for 98889 pedestal.}^2$$

- **Neglecting fueling and variation of V', integrated density equation becomes**

$$\boxed{n_e(\rho)\,\bar{D}_\eta(\rho) \simeq \text{constant} \quad\Longrightarrow\quad n_e(\rho) \simeq n_e(\rho_{\mathrm{REF}})\,\frac{\bar{D}_\eta(\rho_{\mathrm{REF}})}{\bar{D}_\eta(\rho)}, \quad \text{within the pedestal,}}$$

which is density profile needed for outward diffusive flux to be cancelled by pinch flow.

- **Density profile $\sim 1/\bar{D}_\eta \sim f(T_e)$ leads to "aligned" n_e, T_e profiles.**

In 98889 pedestal $n_e(\rho_t)/n_e(\rho_n) \simeq 1.67$ whereas prediction is $n_e(\rho_t)/n_e(\rho_n) \simeq 2.33$.

- **Estimate fueling effects with $\dot{N}_e \simeq \dot{N}_e(a)e^{-(a-\rho)/\lambda_n}$ and assume $\lambda_n > a - \rho$:**

$$\boxed{n_e(\rho)\,\bar{D}_\eta(\rho)\,V'(\rho) \simeq n_e(a)\,\bar{D}_\eta(a)\,V'(a) + \dot{N}_e(a)\,(a-\rho),} \qquad \text{which shifts } n_e \text{ profile}$$

outward relative to T_e profile — like in JET/DIII-D comparison experiments?[6]

[6] M.N.A. Beurkens, T.H. Osborne et al., "Pedestal width and ELM size identity studies in JET and DIII-D ...," PPCF **51**, 124051 (2009).

Pedestal Electron Temperature Profile

- Using density flow equation in electron energy flow equation and neglecting fueling effect $[(3/2)\dot{N}_e T_e/\hat{P}_e \sim 0.025$ in 98889] yields T_e gradient prediction:[1]

$$\boxed{-\frac{dT_e}{d\rho} = \frac{\hat{P}_e(\rho)}{(3/2)\,[V'\bar{D}_\eta\, n_e]} \simeq \text{ constant,}} \quad \text{because } \hat{P}_e \;\&\; [V'\bar{D}_\eta n_e] \simeq \text{constant in pedestal,}$$

which implies that in the pedestal region $\chi_{e\,\mathrm{eff}}^{\mathrm{pc}} = \dfrac{3}{2}\dfrac{a^2}{\bar{a}^2}\dfrac{1}{\langle|\vec{\nabla}\rho|^2\rangle} D_\eta \simeq 1.2\, D_\eta$ (in 98889).

- This predicts the electron temperature gradient scale length ("pedestal width") at the density mid-point is (98889 data[2] indicates $L_{Te}/a \simeq 0.02$):

$$\boxed{\frac{L_{Te}}{a} \equiv \left[-\frac{a}{T_e}\frac{dT_e}{d\rho}\right]^{-1}_{\rho_n} \simeq \frac{(3/2)[V'\bar{D}_\eta\, n_e]_{\rho_n} T_e(\rho_n)}{a\,\hat{P}_e(\rho_n)}} \simeq 0.03, \text{ does not depend on } \rho_*.$$

- Since $\eta_e \gtrsim 2 \gg \eta_{e,\mathrm{crit}} \simeq 1.2$ at top of pedestal, we are in "saturated" ETG regime where anomalous electron heat transport can be represented by[2,7]

$$\chi_e^{\mathrm{ETG}} \simeq f_\# \chi_e^{\mathrm{gB}} \equiv f_\# \frac{\rho_e}{L_{Te}}\frac{T_e}{eB_{\mathrm{t0}}} \simeq 0.075\, f_\# \frac{[T_e(\mathrm{keV})]^{3/2}}{L_{Te}(\mathrm{m})\, B_{\mathrm{t0}}^2(\mathrm{T})^2}\ \mathrm{m^2/s}, \qquad \text{with}^{2,7}\ f_\# \simeq 1.4\text{–}3.$$

- Estimate the pedestal height by equating the ETG heat flow $\Upsilon_{eETG} \simeq -n_e\chi_e^{\mathrm{ETG}} dT_e/d\rho$ to the paleoclassical electron heat flow to obtain[1]

$$\boxed{\beta_e^{\mathrm{ped}} \equiv \frac{n_e^{\mathrm{ped}} T_e^{\mathrm{ped}}}{B_{\mathrm{t0}}^2/2\mu_0} \sim \frac{3\sqrt{2}}{\pi f_\#}\frac{\eta_\parallel^{\mathrm{nc}}}{\eta_0}\frac{L_{Te}}{R_0 q}} \simeq 0.167\text{–}0.36\% \text{ prediction vs. } 0.2\% \text{ in 98889 pedestal.}$$

[7] F. Jenko et al., "Gyrokinetic turbulence under near-separatrix or nonaxisymmetric conditions," Phys. Plasmas **16**, 055901 (2009).

Pedestal Ion Temperature Profile

- **Ion heat transport in H-mode pedestals is apparently a complicated mix of**

  comparable neoclassical and paleoclassical transport throughout the pedestal,

  transition to ITG-driven anomalous transport in the core, and

  kinetic effects in the bottom half of the pedestal, near the separatrix.

- **Neglecting anomalous ion heat transport & kinetic effects, and integrating the ion energy equation as was done for the n_e and T_e equations yields**[1]

$$-\frac{dT_i}{d\rho} \simeq \frac{P_i(\rho)/V'}{(3/2)n_i\bar{D}_\eta + n_i\chi_i^{\rm nc}}, \quad \boxed{\left.\frac{L_{Ti}}{a}\right|_{\rho_n} \equiv \left[-\frac{a}{T_i}\frac{dT_i}{d\rho}\right]^{-1}_{\rho_n} \simeq \frac{[(3/2)\bar{D}_\eta + \chi_i^{\rm nc}]_{\rho_n} n_i(\rho_n)\, T_i(\rho_n)}{a\, P_i(\rho_n)/V'}.}$$

- **Since $n_i\bar{D}_\eta$ and $\chi_i^{\rm nc}$ are often nearly constant in the pedestal, the ion temperature gradient $dT_i/d\rho$ is predicted to be $\sim$ constant in the pedestal.**

- **For the 98889 pedestal $[L_{Ti}/a]_{\rho_n} \simeq 0.06$ versus prediction of 0.12 — maybe both the $\chi_i^{\rm nc}$ and $\chi_i^{\rm pc}$ theoretical values are a bit too large?**[2]

- **Determining "top" of T_i pedestal is problematic because multiple ion heat transport processes are involved and ITG transport is likely near threshold.**

Pedestal Toroidal Flow Profile And Radial Electric Field

- **Poloidal ion flow can be predicted by neo theory: $V_{\mathrm{p}i} \simeq (k_i/q_i B_{\mathrm{t}0})(dT_i/d\rho)$.**

- **Equation for plasma toroidal angular momentum has been derived recently.**[11]

- **Neglecting 3D and microturbulence effects, but including paleoclassical transport and charge-exchange momentum losses $\langle \vec{e}_\zeta \cdot \vec{S}_m \rangle \simeq -\nu_{\mathrm{cx}} L_{\mathrm{t}}$ yields**

$$-\frac{1}{V'}\frac{d^2}{d\rho^2}\left[V'\bar{D}_\eta L_{\mathrm{t}}\right] \simeq -\nu_{\mathrm{cx}} L_{\mathrm{t}}, \quad \text{in which} \quad L_{\mathrm{t}} \equiv m_i n_i \langle R^2 \rangle \Omega_{\mathrm{t}} \text{ is total plasma ang. mom.}$$

- **Neglecting charge-exchange losses and analyzing as for density profile yields**[1]

$$\boxed{\Omega_{\mathrm{t}}(\rho) \simeq \text{constant} \quad \Longrightarrow \quad \Omega_{\mathrm{t}}(\rho) \simeq \Omega_{\mathrm{t}}(a) \quad \text{in pedestal,}} \quad \text{as found in 98889 pedestal.}^{8}$$

- **Adding charge exchange effects and again assuming $\lambda_n > a - \rho$ yields**[1]

$$\Omega_{\mathrm{t}}(\rho) \simeq \Omega_{\mathrm{t}}(a)\left[1 - (a-\rho)\,\lambda_n\,\nu_{\mathrm{cx}}(a)/\bar{D}_\eta(a)\right] \quad \Longrightarrow \quad \text{linearly increasing } \Omega_{\mathrm{t}} \text{ with } \rho.^{9,10}$$

- **Adding ripple effects reduces Ω_{t} in pedestal $\propto \delta B_N^2$, as observed in JET.**[6]

- **Electric field is determined from radial force balance once Ω_{t} is known:**

$$E_\rho = |\vec{\nabla}\rho|\left(\Omega_{\mathrm{t}}\psi'_{\mathrm{p}} + \frac{1}{n_i q_i}\frac{dp_i}{d\rho} - \frac{k_i}{q_i}\frac{dT_i}{d\rho}\right) \simeq |\vec{\nabla}\rho|\frac{1}{n_i q_i}\frac{dp_i}{d\rho} \quad \text{since } \Omega_{\mathrm{t}} \text{ and } \frac{dT_i}{d\rho} \text{ are small.}$$

---

[8] W.M. Stacey, "The effects of rotation, electric field, and recycling neutrals on determining the edge pedestal density ...," PoP **17**, 052506 (2010).
[9] J.S. deGrassie, J.E. Rice, K.H. Burrell. R.J. Groebner, and W.M. Solomon, "Intrinsic rotation in DIII-D," PoP **14**, 056115 (2007).
[10] T. Pütterich et al., "Evidence for Strong Inversed Shear of Toroidal Rotation at the Edge-Transport Barrier in AUG," PRL **102**, 025001 (2009).

Regime: **Paleoclassical Transport Likely Dominates At Low T_e**

- **Since $D_\eta \propto \eta \propto 1/T_e^{3/2}$, $\chi_e^{\rm pc}$ in the confinement region (I) is typically**

$$\chi_{eI}^{\rm pc} \sim \frac{Z_{\rm eff}\,[\bar{a}(\rm m)]^{1/2}}{[T_e(\rm keV)]^{3/2}}\,\frac{\rm m^2}{\rm s} \;\gtrsim\; 1\ {\rm m^2/s}\ \text{for}\ T_e \lesssim 2\ {\rm keV}.$$

- **Microturbulence-induced transport usually has a gyroBohm scaling:**

$$\text{ITG, DTE:}\ \ \chi_e^{\rm gB} \equiv f_\# \frac{\varrho_s}{a}\frac{T_e}{eB} \simeq 3.2 f_\# \frac{[T_e(\rm keV)]^{3/2} A_i^{1/2}}{\bar{a}(\rm m)\,[B(\rm T)]^2}\,\frac{\rm m^2}{\rm s} \;\gtrsim\; 1\ {\rm m^2/s}\ \text{for}\ T_e \gtrsim 0.5\ {\rm keV}/f_\#^{2/3},$$

in which $f_\#$ is a threshold-type factor that depends on magnetic shear, T_e/T_i, ν_{*e} etc.

- **Thus, paleoclassical electron heat transport is likely dominant at low T_e:**

$$T_e \lesssim \boxed{T_e^{\rm crit} \equiv [B(\rm T)]^{2/3}[\bar{a}(\rm m)]^{1/2}/(3f_\#)^{1/3}\ \rm keV} \sim 0.6\text{–}2.4\ {\rm keV}\ (f_\# \sim 1/3),\ \text{present expt.}$$

- **In DIII-D the electron temperature T_e in the H-mode pedestal ranges from about 100 eV at the separatrix to about 1 keV at top of pedestal**

  $\Longrightarrow$ **paleoclassical $\chi_e^{\rm pc}$ is likely to be dominant in DIII-D H-mode pedestal region.**

- **In ITER $T_e^{\rm crit} \sim 3.5$–5 keV $\Longrightarrow$ paleoclassical may be dominant for ITER ohmic startup and in the pedestal region?**

Paleoclassical Effects Occur In All Transport Channels

- *Density* of a species s (electrons and all ions — intrinsically ambipolar):[11]

$$\Gamma_s^{\rm pc} \equiv -\frac{1}{V'}\frac{\partial}{\partial\rho}(V'\bar{D}_\eta n_{s0}) = -\bar{D}_\eta\frac{\partial n_{s0}}{\partial\rho} + n_{s0}V_{\rm pc}, \qquad \boxed{V_{\rm pc} \equiv -\frac{1}{V'}\frac{\partial}{\partial\rho}(V'\bar{D}_\eta) \sim -\frac{3\,\bar{D}_\eta}{2\,L_{Te}}.}$$

- *Electron heat transport* has a different transport operator:[12]

$$\langle\vec{\nabla}\cdot\vec{Q}_e^{\rm pc}\rangle = -\frac{M+1}{V'}\frac{\partial^2}{\partial\rho^2}\left(V'\bar{D}_\eta\frac{3}{2}n_eT_e\right), \quad \text{with} \quad M \simeq \frac{\lambda_e}{\pi R_0 q} \sim 3\searrow 0 \text{ in pedestal region.}$$

- *Ion heat transport flux* is similar[12] to density transport:

$$\Upsilon_s^{\rm pc} \equiv -\frac{1}{V'}\frac{\partial}{\partial\rho}\left(V'\bar{D}_\eta\frac{3}{2}n_{i0}T_{i0}\right) = -\bar{D}_\eta\frac{\partial}{\partial\rho}\left(\frac{3}{2}n_{i0}T_{i0}\right) + \frac{3}{2}n_{i0}T_{i0}V_{\rm pc}.$$

- *Toroidal momentum radial transport* is similar[11] to density and ion heat transport ($L_t \equiv m_i n_{i0}\langle R^2\Omega_t\rangle$, FSA plasma toroidal angular momentum density):

$$\Pi_{\rho\zeta}^{\rm pc} \equiv -\frac{1}{V'}\frac{\partial}{\partial\rho}(V'\bar{D}_\eta L_t) = -\bar{D}_\eta\frac{\partial L_t}{\partial\rho} + L_t V_{\rm pc}.$$

- Pinch effects from $V_{\rm pc}$ are caused by structure of paleo transport operators — because $\langle(\Delta x_g)^2\rangle/2\Delta t = \bar{D}_\eta$ but $\langle\Delta x_g\rangle/\Delta t \simeq 0$ for paleo processes.

[11] J.D. Callen, A.J. Cole, and C.C. Hegna, "Toroidal flow and radial particle flux in tokamak plasmas," Phys. Plasmas **16**, 082504 (2009).
[12] J.D. Callen, C.C. Hegna, and A.J. Cole, "Transport equations in tokamak plasmas," Phys. Plasmas **17**, 056113 (2010).

Pedestal Trapped, Circulating Particle Effects Are Complex

- **The usual definition of the electron neoclassical collisionality parameter is**

$$\nu_{*e} = \frac{\nu_e}{\epsilon^{3/2} v_{Te}/R_0 q} = \frac{R_0 q}{\epsilon^{3/2}\lambda_e}, \quad \text{for } \sqrt{\epsilon} \ll 1 \quad \text{(i.e., in the large aspect ratio expansion).}$$

- **However, in developing multi-collisionality formulas for the neoclassical parallel resistivity (p 5), relevant neoclassical collisionality parameter is**[13,14]

$$\nu_{*e} = \frac{f_t/f_c}{2.92}\,\frac{\nu_e}{v_{Te}R_0 q}\,\frac{\langle B_0^2\rangle}{\langle(\hat{\vec{b}}\cdot\vec{\nabla}B_0)^2\rangle} \simeq \frac{f_t/f_c}{1.46\epsilon^2}\,\frac{R_0 q}{\lambda_e}; \quad \text{hence,} \quad \frac{1}{\epsilon^{3/2}} \Longrightarrow \frac{f_t/f_c}{1.46\epsilon^2} \text{ in } \nu_{*e}.$$

- **This changes the pedestal collisionality in low A tokamaks significantly:**

  DIII-D: $\epsilon \simeq 0.35$; $f_t/f_c \simeq 0.77/0.23 \simeq 3.35$, **which increases** ν_{*e} **by a factor of 3.88.**

  NSTX: $\epsilon \simeq 0.65$; $f_t/f_c \simeq 0.93/0.07 \simeq 13.3$, **which increases** ν_{*e} **by a factor of 11.3.**

- **For DIII-D this reduces earlier** $\eta_\parallel^{\rm nc}/\eta_0$ **values to 0.64 at** ρ_n **and 0.81 at** ρ_t**, modifies pedestal structure model predictions and shows importance of** $\eta_\parallel^{\rm nc}$**.**

- **New** ν_{*e} **and** $Z_{\rm eff}$ **profile are critical for comparisons of this pedestal structure model to NSTX data with/without Li — see J. Canik, JI2.1 invited talk viewgraph # 20 at 2010 DPP-APS Chicago meeting.**[3]

[13] Y.B. Kim, P.H. Diamond and R.J. Groebner, Phys. Fluids B **3**, 2050 (1991); Erraturm, Phys. Fluids B **4**, 2996 (1992).
[14] J.D. Callen, "Viscous Forces Due To Collisional Parallel Stresses For Extended MHD Codes," UW-CPTC 09-6R, Feb. 4, 2010; Ref. [11] in ref**12**.

98889 Pedestals: ***Transport Quasi-equilibrium Will Be Studied***

- **LSN DIII-D 98889 discharge has:**[2]

  $P_{\rm NBI} \simeq 2.91$ MW,

  $P_{\rm OH} \simeq 0.3$ MW,

  $B_{\rm t0} \simeq 2$ T,

  $I \simeq 1.2$ MA,

  $q_{95} \simeq 4.4$,

  $a \simeq 0.77$ m,

  mid-plane half-radius $r_M \simeq 0.6$ m,

  low $n_e^{\rm ped}$, high $T_e^{\rm ped}$.

- **Transport question to be addressed is:**

  Can initial ($\sim$ 10 ms), transport-limited, quasi-equilibrium pedestal structure be predicted?

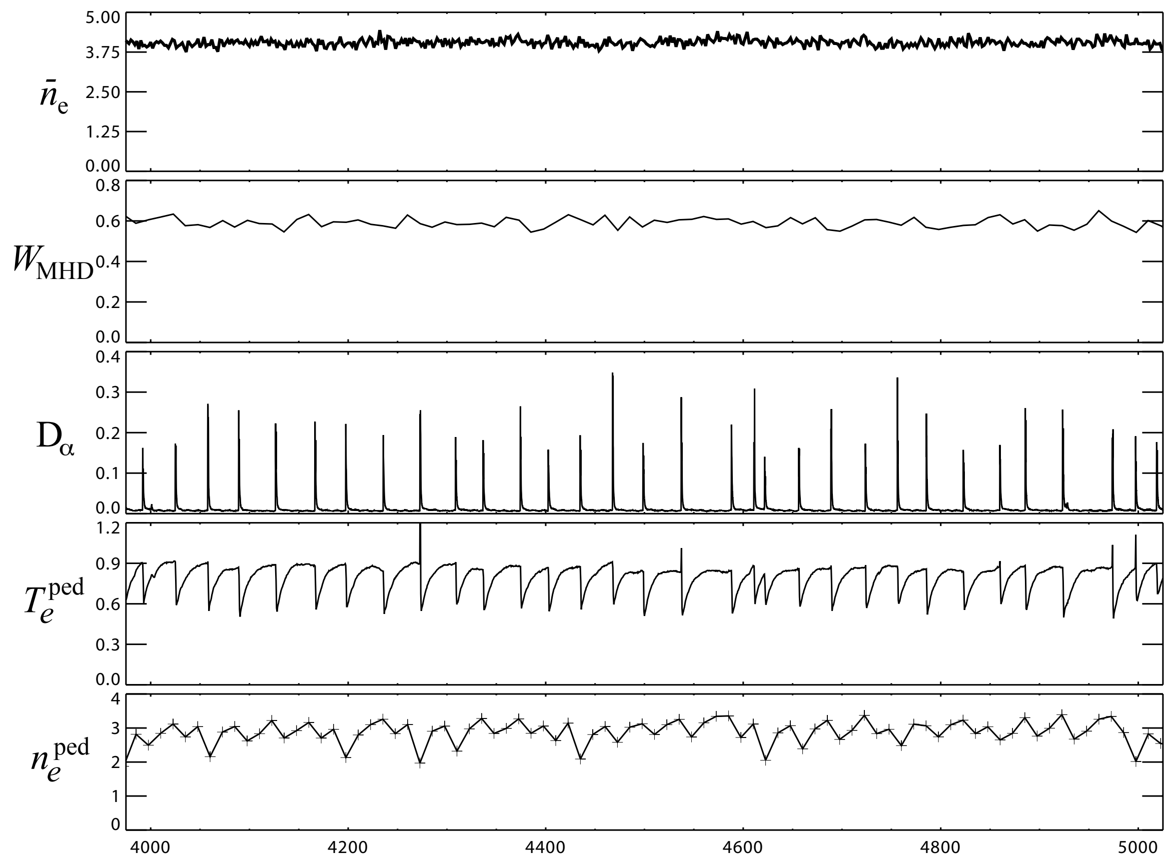

Figure 5: **T_e and n_e profiles recover quickly ($\sim$ 10 ms) after ELM, then evolve slowly ($\sim$ 25 ms) to next ELM. Quasi-equilibrium profiles are obtained by binning 80–99% data of ELM cycles, averaging over 4–5 s.**[2]

Paleoclassical Density Transport Model Roughly Agrees With New Procedure Results For Pinch And “True” D_{exp}

- **Pinch flow is large in pedestal,[5] cancels $\sim$ 90 % of diffusive flux in II, III.**
- **“True” pinch-corrected D_{exp} is very different;[5] V_{pinch} & D_{exp} $\sim$ paleo model.[15]**
- **Pedestal n_e transport barrier is artifact of neglecting pinch in inferring D.**

[15] See Eq. (125) in J.D. Callen, A.J. Cole, C.C. Hegna, “Toroidal flow and radial particle flux in tokamak plasmas,” Phys. Pl. **16**, 082504 (2009).

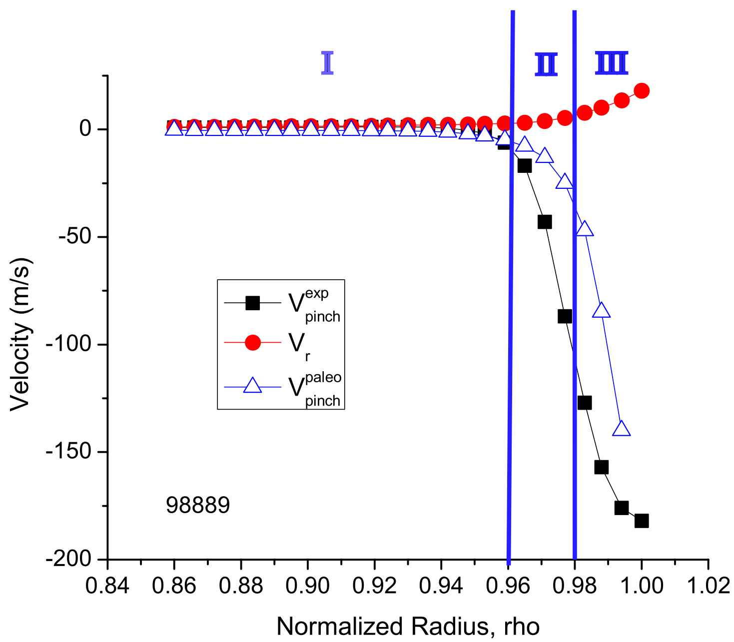

Figure 6: **GTEDGE radial flow velocities[5] from: new pinch flow procedure (black squares), net (○), and paleo pinch (△).**

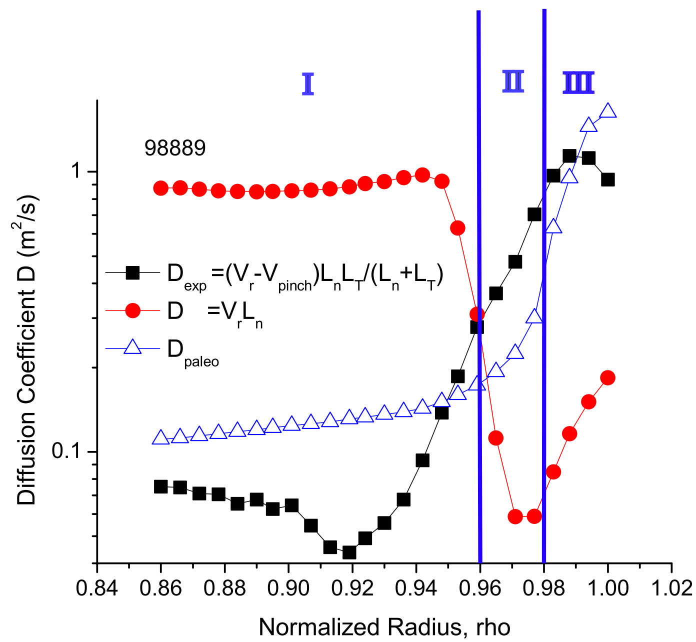

Figure 7: **GTEDGE particle diffusivities:[5] usual D (○ circles), “true” $D_{\text{exp}} \equiv D_i$ corrected for pinch (black squares) and paleo D_{paleo} (△).**